

Formation of nanostructured TiO₂ by femtosecond laser irradiation of titanium in O₂

Elizabeth C. Landis,¹ Katherine C. Phillips,² Eric Mazur,² and Cynthia M. Friend^{1,2}

¹*Department of Chemistry, Harvard University, 12 Oxford Street, Cambridge, Massachusetts 02138, USA*

²*School of Engineering and Applied Sciences, Harvard University, 9 Oxford Street, Cambridge, Massachusetts 02138, USA*

(Received 24 July 2012; accepted 9 August 2012; published online 18 September 2012)

We used femtosecond laser irradiation of titanium metal in an oxidizing environment to form a highly stable surface layer of nanostructured amorphous titanium dioxide (TiO₂). We studied the influence of atmospheric composition on these surface structures and found that gas composition and pressure affect the chemical composition of the surface layer but not the surface morphology. Incorporation of nitrogen is only possible when no oxygen is present in the surrounding atmosphere. © 2012 American Institute of Physics. [<http://dx.doi.org/10.1063/1.4752276>]

INTRODUCTION

Femtosecond laser pulses provide a way to simultaneously structure and change the chemical composition of a number of materials, including titanium.^{1–3} Laser structuring of titanium surfaces has been investigated because the topography of the titanium surface contributes to its biocompatibility,⁴ tribology, and hydrophobicity.⁵ Femtosecond lasers have been used to produce a wide variety of surface structures on titanium including conical microstructures,⁶ periodic gratings,⁷ and nanoscale pores.⁸

Laser processing also makes it possible to insert nitrogen and oxygen atoms into titanium while creating surface structures.^{9,10} Experiments involving titanium surfaces irradiated by nanosecond lasers show that the surrounding gas atmosphere can have a large impact on the surface chemical composition and the surface morphology.¹¹

Because titanium, known for its durability, mechanical properties, and stability, is used in many biomedical applications,¹² the effect of laser irradiation on biocompatibility is particularly important. While surface structures enhance cell adhesion,¹³ the chemical composition of structured titanium surfaces also contributes to their biocompatibility. For example, the biocompatibility of titanium is improved by a thin layer of TiO₂ on the surface of a titanium implant.¹⁴ Nitridation of titanium also has applications in biomaterials and microdevices for improvements in wear resistance and hardening.¹²

Although a high degree of control over femtosecond laser-formed titanium surface morphologies has been developed, the chemical composition of the resulting films has not been studied in detail. In this work, we investigate the influence of oxygen and nitrogen gas composition on the surface morphology, chemical composition, and stability of femtosecond laser irradiated titanium surfaces.

EXPERIMENTAL

Samples were produced by irradiating a 99.99% titanium plate with a 25–33.33 Hz train of 100 fs, 805 nm laser pulses from an amplified Ti:sapphire laser. The pulses have a fluence of 2.5 kJ/m² and are polarized in the *x* direction (*x*-y

axes shown in Figure 1).¹⁵ The samples were mounted on an *x*-y stage in a stainless steel chamber that was evacuated to less than 0.1 Torr and then filled with a background gas. To irradiate the sample, we raster scan in the *x* direction and step in the *y* direction at the end of each row, uniformly exposing each spot on the sample to 50 laser pulses.

Images of the samples were taken with a Zeiss Ultra55 scanning electron microscope (SEM) with a beam energy of 2 keV. Elemental analysis was performed using x-ray photoelectron spectroscopy (XPS), which we collected on a Surface Science SSX-100 ESCA spectrometer. Ar⁺ sputtering was used for cleaning and depth profiling analysis at 2.7 keV. Survey spectra were collected with an 800 nm spot size at 1 eV per step and high-resolution scans with a 300 nm spot size at 0.065 eV per step. We then performed XPS peak fitting using Casa XPS, and peaks were fit with Shirley background-corrected Lorentzian functions.

X-ray diffraction data (XRD) were collected on a Bruker D8 Discover. The XRD experiments are performed on samples made from a 450 nm thick layer of titanium, evaporated onto a glass slide to minimize background from the unstructured underlying titanium and then irradiated with the same conditions detailed above. We collected Raman spectroscopy on a Renishaw inVia microscope using an excitation wavelength of 633 nm, produced by a 5 mW, s-polarized Helium-Neon laser. The Raman spectra were recorded through a 50 × microscope objective, which was projected onto a thermoelectrically cooled, charged-coupled device (CCD) array using a 1200 groove/mm diffraction grating.

Electrochemistry data were collected using a CH Instruments Electrochemical Analyzer CHI600D. We used a three-electrode setup with the untreated and treated titanium surfaces individually isolated as the working electrode, a BASi Ag/AgCl reference electrode, and a Pt coil counter electrode. The electrochemical cell was filled with an electrolyte, BioWhittaker Hanks' balanced salt solution, which was purged with argon for 60 min before use. All measurements were performed at room temperature.

Reflectivity measurements were taken with a Hitachi U-4100 spectrophotometer with a BaSO₄ integrating sphere.

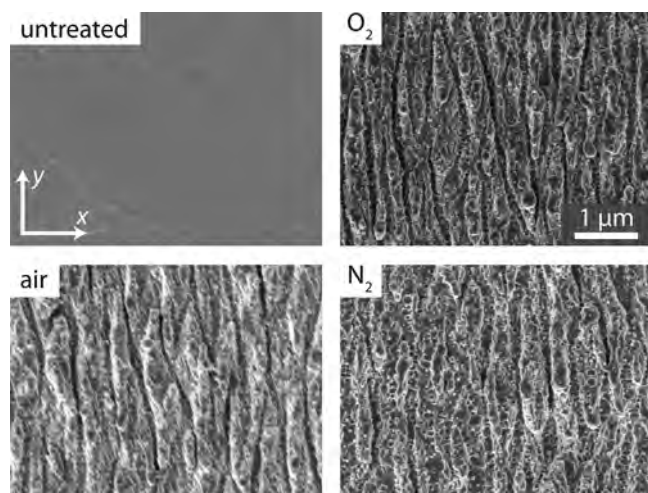


FIG. 1. Scanning electron micrographs of titanium metal surface before (untreated) and after laser irradiation in the ambient gases shown, with a total pressure of 100 Torr in each case. The air mixture consists of a 1:4 ratio of $O_2:N_2$.

RESULTS AND DISCUSSION

SEM images of the films irradiated with a total atmospheric pressure of 100 Torr (Figure 1) show laser-induced periodic surface structures (LIPSS)¹⁶ that do not vary with the atmospheric composition of oxygen and nitrogen. The lines of the grooved pattern are oriented along the y direction, perpendicular to the laser polarization. This grooved pattern of the LIPSS is expected for near-damage-threshold laser fluences and multiple laser pulses.¹⁷ The formation of LIPSS on metals has been attributed to the interference of the incident laser light with excited surface plasmon polaritons.¹⁸ Varying the total pressure of oxygen and nitrogen between 0.01 and 500 Torr does not change the surface morphology of the titanium structures. The same surface structures are visible after irradiation with 1, 10, or 50 laser pulses, regardless of the chemical composition of the background atmosphere.

Fourier transformations of the periodic surface structures confirm that samples formed in different atmospheric conditions all have a periodicity of 268 ± 15 nm. The periodicity of the surface grating formed from the interference between the incident laser light and excited surface plasmon wave is λ/n , where λ is the wavelength of the incident light and n is the index of refraction.¹⁹ The index of refraction of titanium at 805 nm is 2.883, producing a periodicity of 279.2 nm, in agreement with the measured periodicity of 268 ± 15 nm.

The XPS spectra in Figure 2 show that the ambient gas composition and pressure affect the chemical composition, and hence the physical properties, of the titanium surface structures. Surfaces irradiated in atmospheres containing only oxygen show significant amounts of only titanium and oxygen with more oxygen incorporated than in the untreated films. The films were measured after argon sputtering to remove surface atoms and reveal subsurface composition. The chemical shift of the Ti 2p peaks, shown in Figure 2(b), can be used to identify the oxidation state of the titanium atoms. The sample structured in 100 Torr oxygen has Ti 2p_{3/2} and Ti 2p_{1/2} peaks

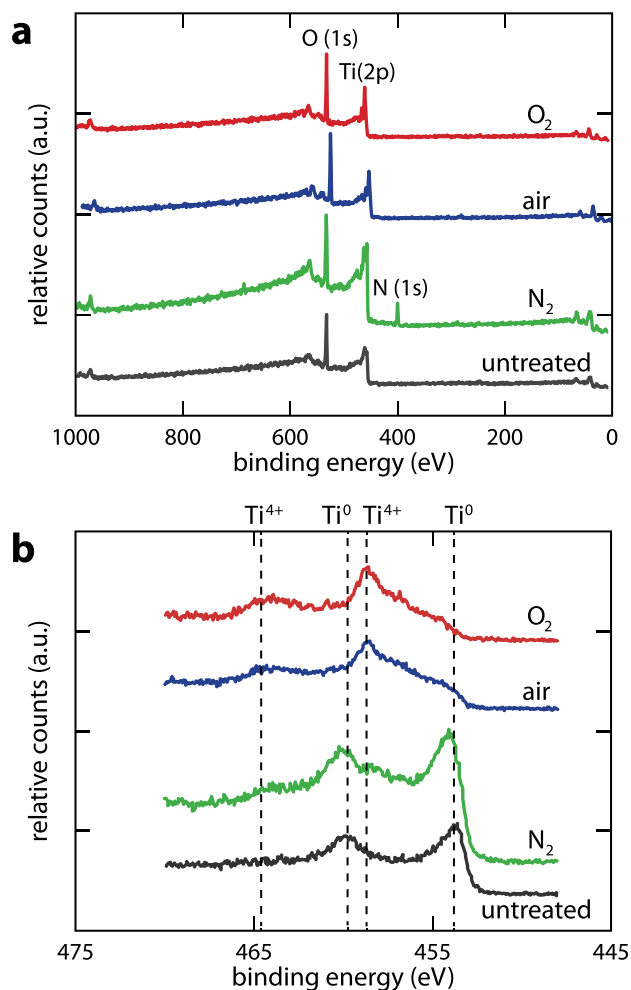


FIG. 2. (a) XPS of untreated titanium and laser-structured samples. The samples were Ar^+ sputtered for 10 min immediately before measurement. (b) High resolution XPS of the Ti (2p) region of untreated and laser-structured titanium. The samples were Ar^+ sputtered for 20 min before measurements.

at 458.7 and 464.6 eV, respectively, which correspond to Ti^{4+} , the oxidation state found in TiO_2 .²⁰

TiO_2 forms as a native oxide on titanium metal, so we compare our results to an argon sputtered, untreated titanium sheet. The untreated titanium control has Ti 2p_{3/2} and Ti 2p_{1/2} peaks at 453.8 and 459.8 eV, which correspond to metallic titanium and confirm that the argon sputtering treatment is sufficient to remove the native oxide layer. The O:Ti ratio for a film structured in 100 Torr O_2 is 2.3 before argon sputtering treatment and 1.9 after 10 min of sputtering, which shows that the sputtering differentially removes oxygen atoms. To quantify the bulk reduction caused by the argon ion sputtering, we also compared the laser-oxidized samples to a sputter deposited TiO_2 thin film. The sputter-deposited TiO_2 film is slightly more reduced following the argon sputtering treatment than the TiO_2 films formed by irradiating in oxidizing atmospheres after the same treatment. This may indicate that the sputter deposited TiO_2 film is thinner than the irradiated films. This observation, combined with the predominant Ti^{4+} oxidation state, shows that laser irradiation of titanium metal in an oxidizing atmosphere forms a surface layer of TiO_2 . Due to the

bulk reduction caused by sputtering, it is difficult to quantify the presence of additional titanium oxidation states in the laser-structured samples. While predominantly TiO_2 , it is possible that the samples also contain smaller amounts of the less oxidized Ti_2O_3 or TiO .

As shown in Figure 2(a), titanium surfaces irradiated in a nitrogen atmosphere contain titanium, oxygen, and nitrogen. The amount of nitrogen does not decrease with argon sputtering, showing that it is incorporated into the titanium lattice. By integrating the area under the peaks, we found that the N:Ti ratio is 0.34. The samples formed in only nitrogen have Ti $2p_{3/2}$ and $2p_{1/2}$ peaks at 454.1 and 460.0 eV, 0.2 eV higher than the untreated titanium control. The expected binding energy for Ti in TiN is 1.4 eV higher than the measured values. Previous studies of non-stoichiometric titanium nitride films with low nitrogen incorporation show Ti binding energies 0.3–0.4 eV above metallic Ti, similar to our samples.¹¹ Analysis of nitrogen incorporation as a function of nitrogen pressure incorporated during irradiation shows a slight decrease in nitrogen incorporation with decreasing nitrogen pressure. Nitrogen is only incorporated into the titanium lattice when surface structures are created, implying that the laser fluence necessary for nitrogen incorporation is above the melting threshold.

Titanium samples irradiated in 80 Torr N_2 and 20 Torr O_2 , a composition approximating air, show incorporation of oxygen but not nitrogen. These samples also show the same Ti $2p$ peak placement as the sample irradiated in only oxygen, indicating the formation of TiO_2 . We find that the presence of 0.1 Torr of oxygen in the chamber prevents the incorporation of nitrogen into the sample. The preferential formation of TiO_2 over TiN can be explained by considering the relative heats of formation (Δ_{fH}) of the bulk materials. While the formation of both structures is exothermic, the heat of formation of TiO_2 is $\Delta_{\text{fH}} = -944.0$ kJ/mol, while the formation of TiN is less favorable at $\Delta_{\text{fH}} = -337.7$ kJ/mol.^{12,21}

We analyzed the crystal structure of the resulting films using both Raman spectroscopy and XRD. XRD of the unstructured titanium film in Figure 3 shows the characteris-

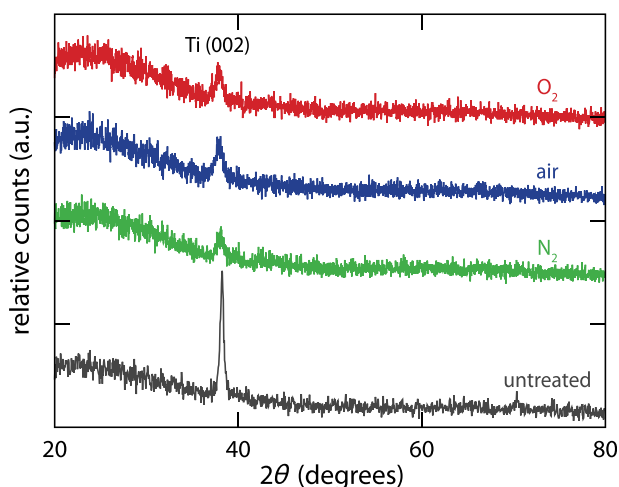


FIG. 3. XRD of the untreated titanium and laser-structured samples. The films display only the (002) and (103) peaks expected for evaporated titanium.

tic peaks of α -Ti with a strong (002) peak at $2\theta = 38.3^\circ$ and a smaller (103) reflection peak at 70.6° . This structure is expected for evaporated titanium films.²² The laser structured samples do not show additional peaks that would indicate the presence of crystalline TiO_2 or TiN. We would expect peaks at $2\theta = 25.3^\circ$ and 48.2° for anatase TiO_2 or at 27.5° and 54.3° for rutile TiO_2 .²³ The structured films do have a small Ti (002) peak, which can be attributed to the underlying unstructured titanium.

Raman spectroscopy confirms the amorphous nature of the structured films. As shown in Figure 4, the samples structured in oxygen or air to form TiO_2 display a single broad peak at 240 cm^{-1} with a smaller broad hump around 450 cm^{-1} . The broad spectrum is consistent with an amorphous semiconductor. The peaks may be due to the presence of Ti_2O_3 because crystalline Ti_2O_3 has peaks at 269, 302, 347, and 452 cm^{-1} .²⁴ Spectra of few nm thick oxidized titanium films display similar broad peaks that have been attributed to a thin layer of Ti_2O_3 .²⁵ These peaks indicate the presence of Ti_2O_3 species within the predominant TiO_2 shown in the XPS spectra. The presence of less oxidized species may be caused by preferential ablation of lighter oxygen atoms during laser irradiation. The absence of peaks at 447 and 612 cm^{-1} indicates that rutile TiO_2 is not present; similarly, anatase TiO_2 would lead to peaks at 144, 197, 399, 515, and 639 cm^{-1} , which are not observed.²³

The sample structured in nitrogen resulting in non-stoichiometric TiN has broad Raman peaks at 240 cm^{-1} , 300 cm^{-1} , and 550 cm^{-1} . These are the expected peak positions for non-stoichiometric TiN; the lower-frequency peaks are attributed to acoustic phonons and the high frequency peak at 550 cm^{-1} is attributed to optical phonons.²⁶ The peak positions are very similar to those observed for non-stoichiometric TiN formed by ns-laser irradiation of titanium in a nitrogen environment.²⁷ The Raman spectrum for the unstructured titanium film shows no significant peaks as expected.

Electrochemical stability tests performed in a solution used to simulate biocompatibility¹⁹ demonstrate the stability of the TiO_2 films and their suitability for biological implants.

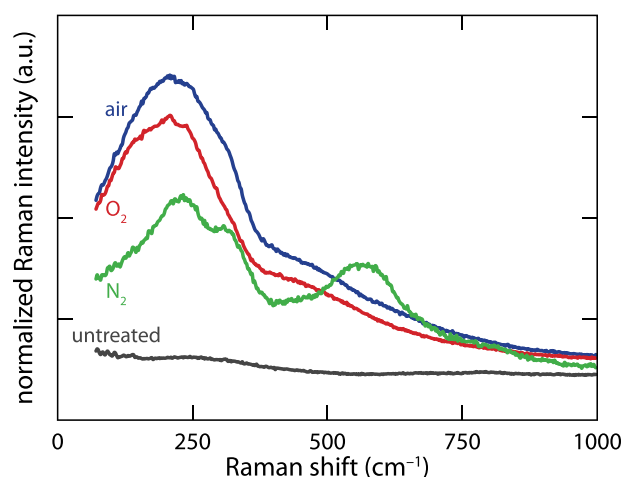


FIG. 4. Raman spectra of the untreated titanium and laser-structured samples, collected from an excitation wavelength of 633 nm.

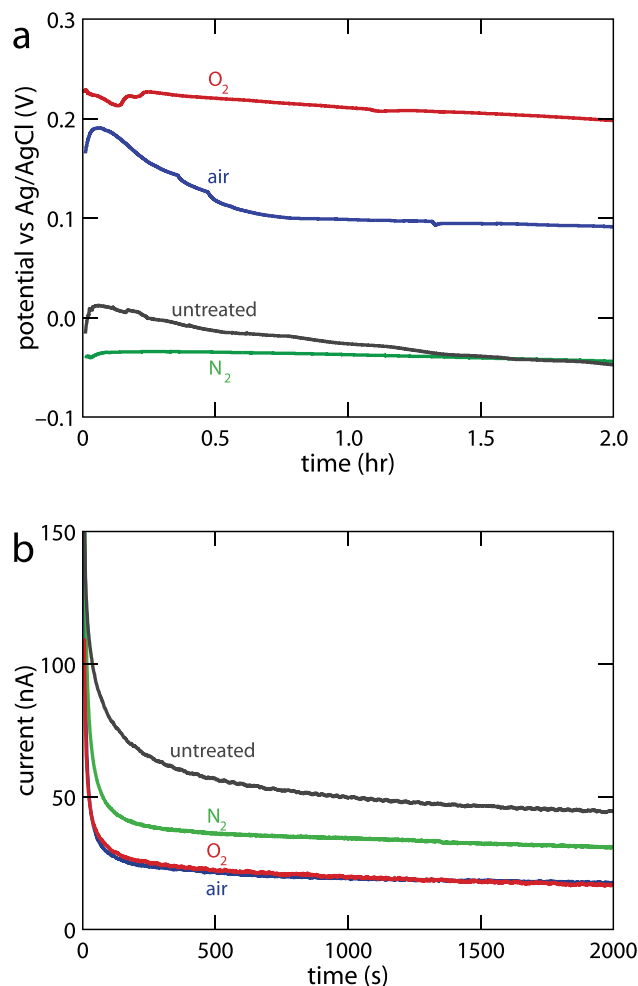


FIG. 5. (a) Open circuit measurements before and after laser irradiation collected at room temperature in a solution to simulate biocompatibility, measured vs. NHE. (b) Current density changes of untreated and laser-structured samples at 494 mV (vs. NHE).

For metal-based films, a high open circuit potential (OCP) indicates increased stability against oxidation. After 2 h of stabilization, the samples irradiated in 100 Torr O₂ and 80 Torr N₂/20 Torr O₂ have open circuit potentials of 0.199 V and 0.092 V (vs. normal hydrogen electrode, NHE),²⁸ respectively (Figure 5(a)). Both oxidized samples have a higher OCP than the titanium plate, which has an OCP of -0.044 V, indicating their higher stability against oxidation. On the other hand, the sample structured in nitrogen shows lower stability against oxidation than the titanium plate with an OCP of -0.061 V.

We also measured the stability of the samples by applying a potential difference of 494 mV (vs. NHE), which is a standard benchmark for dental implant stability. Lower current densities are indicative of higher stability against chemical reactions such as ion release, and thus a higher stability of the oxidized films. As shown in Figure 5(b), we observe an immediate decrease in current when the potential is applied, indicating the formation of a passivation layer. The current of the laser-irradiated films stabilizes after about 10 min, and the oxidized films formed in both air and oxygen stabilize at current densities of 86 nA/cm². The titanium nitride films stabilize at a higher current density of 150 nA/cm². The unstructured titanium surface has the highest current density

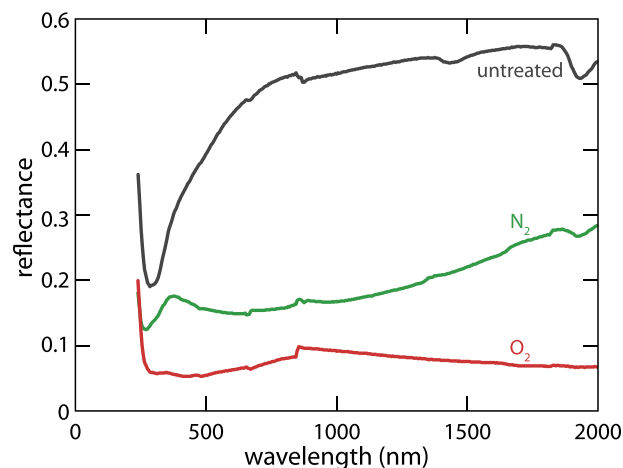


FIG. 6. Reflectivity of samples measured with a spectrophotometer with an integrating sphere.

of 220 nA/cm² and takes longer than the irradiated films to stabilize, indicating that the passivation layer forms more slowly.

Because the surface morphology does not depend on gas composition and pressure, the chemical composition of the surface can be changed independently of the surface morphology. Our findings are in contrast to earlier published work, showing a strong dependence of the surface morphology on gas composition and pressure when titanium is irradiated with nanosecond pulses below the ablation threshold.¹¹ (The chemical composition of the surface structures was not investigated.) As Figure 6 shows, the reflectivity of the samples irradiated by femtosecond pulses does depend on gas composition—untreated titanium and surfaces irradiated in nitrogen and oxygen all have different reflectivities. Our work thus shows that femtosecond laser irradiation makes it possible to create films of varying chemical composition and optical properties while maintaining consistent surface structures.

In conclusion, we form nanostructured TiO₂ and non-stoichiometric TiN films by femtosecond laser irradiation of titanium in oxygen and nitrogen, respectively. We demonstrate that oxygen and nitrogen are incorporated in these films when the laser fluence exceeds the ablation threshold. Furthermore, laser-formed TiO₂ is more stable than untreated titanium in biologically relevant solutions, making femtosecond laser-formed TiO₂ a good candidate for biomedical devices.

ACKNOWLEDGMENTS

Several people contributed to the work described in this paper. E.C.L. and K.C.P. carried out the experiments and prepared the manuscript. E.M. and C.F. supervised the research. The authors thank Anne Co and Meng-Ju Sher for assistance with preliminary experiments and Rafael Jaramillo for assistance with the XRD measurements. The research described in this paper was supported by the National Science Foundation under Contract No. CHE-DMR-DMS 0934480. E.C.L. acknowledges support from the Henson Fund at the Harvard Center for the Environment.

K.C.P. acknowledges support from the National Science Foundation Graduate Research Fellowship under Grant Nos. DGE 0644491 and DGE 0946799 and the Department of Defense (DoD) through the National Defense Science and Engineering Graduate Fellowship (NDSEG) Program.

- ¹B. N. Chichkov, C. Momma, S. Nolte, F. von Alvensleben, and A. Tünnermann, *Appl. Phys. A* **63**, 109–115 (1996).
- ²A. Gaggli, G. Schultes, W. D. Müller, and H. Kärcher, *Biomaterials* **21**, 1067–1073 (2000).
- ³A. Semerok, C. Chaleard, V. Detalle, J.-L. Lacour, P. Mauchien, P. Meynadier, C. Nouvellon, B. Salle, P. Palianov, M. Perdrix, and G. Petite, *Appl. Surf. Sci.* **138–139**, 311–314 (1999).
- ⁴R. G. Flemming, C. J. Murphy, G. A. Abrams, S. L. Goodman, and P. F. Nealey, *Biomaterials* **20**, 573–588 (1999).
- ⁵S. Tugulu, K. Löwe, D. Scharnweber, and F. Schlottig, *J. Mater. Sci.: Mater. Med.* **21**, 2751–2763 (2010).
- ⁶B. K. K. Nayak, M. C. C. Gupta, and K. W. W. Kolasinski, *Appl. Phys. A* **90**, 399–402 (2008).
- ⁷K. Okamuro, M. Hashida, Y. Miyasaka, Y. Ikuta, S. Tokita, and S. Sakabe, *Phys. Rev. B* **82**, 165417 (2010).
- ⁸A. Vorobyev and C. Guo, *Appl. Surf. Sci.* **253**, 7272–7280 (2007).
- ⁹N. Ohtsu, K. Kodama, K. Kitagawa, and K. Wagatsuma, *Appl. Surf. Sci.* **255**, 7351–7356 (2009).
- ¹⁰N. Ohtsu, K. Kodama, K. Kitagawa, and K. Wagatsuma, *Appl. Surf. Sci.* **256**, 4522–4526 (2010).
- ¹¹E. György, A. Pérez del Pino, P. Serra, J. L. Morenza, E. György, and A. Pérez del Pino, *Surf. Coat. Technol.* **187**, 245–249 (2004).
- ¹²D. M. Brunette, P. Tengvall, and M. Textor, *Titanium in Medicine* (Springer-Verlag, Berlin, 2001).
- ¹³B. D. Boyan, T. W. Hummert, D. D. Dean, and Z. Schwartz, *Biomaterials* **17**, 137–146 (1996).
- ¹⁴L.-H. Li, Y.-M. Kong, H.-W. Kim, Y.-W. Kim, H.-E. Kim, S.-J. Heo, and J.-Y. Koak, *Biomaterials* **25**, 2867–2875 (2004).
- ¹⁵B. Tull, Ph.D. dissertation, Harvard University, 2007.
- ¹⁶M. J. Sher, M. T. Winkler, and E. Mazur, *MRS Bull.* **36**, 439–445 (2011).
- ¹⁷C. Wang, H. Huo, M. Johnson, M. Shen, and E. Mazur, *Nanotechnology* **21**, 075304 (2010).
- ¹⁸J. Sipe, J. Young, J. Preston, and H. van Driel, *Phys. Rev. B* **27**, 1141–1154 (1983).
- ¹⁹P. A. Temple and M. J. Soileau, *IEEE J. Quantum Electron.* **17**, 2067–2072 (1981).
- ²⁰See supplementary material at <http://dx.doi.org/10.1063/1.4752276> for information on XPS peak fitting.
- ²¹M. W. Chase, *J. Phys. Chem. Ref. Data Monogr.* **9**, 1–1951 (1998).
- ²²K. Cai, M. Muller, J. Bossert, A. Rechtenbach, and K. D. Jandt, *Appl. Surf. Sci.* **250**, 252–267 (2005).
- ²³J. Zhang, M. Li, Z. Feng, J. Chen, and C. Li, *J. Phys. Chem. B* **110**, 927–935 (2006).
- ²⁴A. Mooradian and P. M. Raccach, *Phys. Rev. B* **3**, 4253 (1971).
- ²⁵R. Nemanich, C. Tsai, and G. Connell, *Phys. Rev. Lett.* **44**, 273–276 (1980).
- ²⁶W. Spengler, R. Kaiser, A. N. Christensen, and G. Muller-Vogt, *Phys. Rev. B* **17**, 1095–1101 (1978).
- ²⁷E. György, A. Pérez del Pino, P. Serra, and J. L. Morenza, *Appl. Surf. Sci.* **186**, 130–134 (2002).
- ²⁸A. J. Bard and L. R. Faulkner, *Electrochemical Methods* (John Wiley & Sons, New York, 1980), p. 2.